VIP Photochemistry

DOI: 10.1002/ange.201103557

Conjugation of Porphyrin to Nanohybrid Cerasomes for Photodynamic Diagnosis and Therapy of Cancer**

*Xiaolong Liang, Xiaoda Li, Xiuli Yue, and Zhifei Dai**

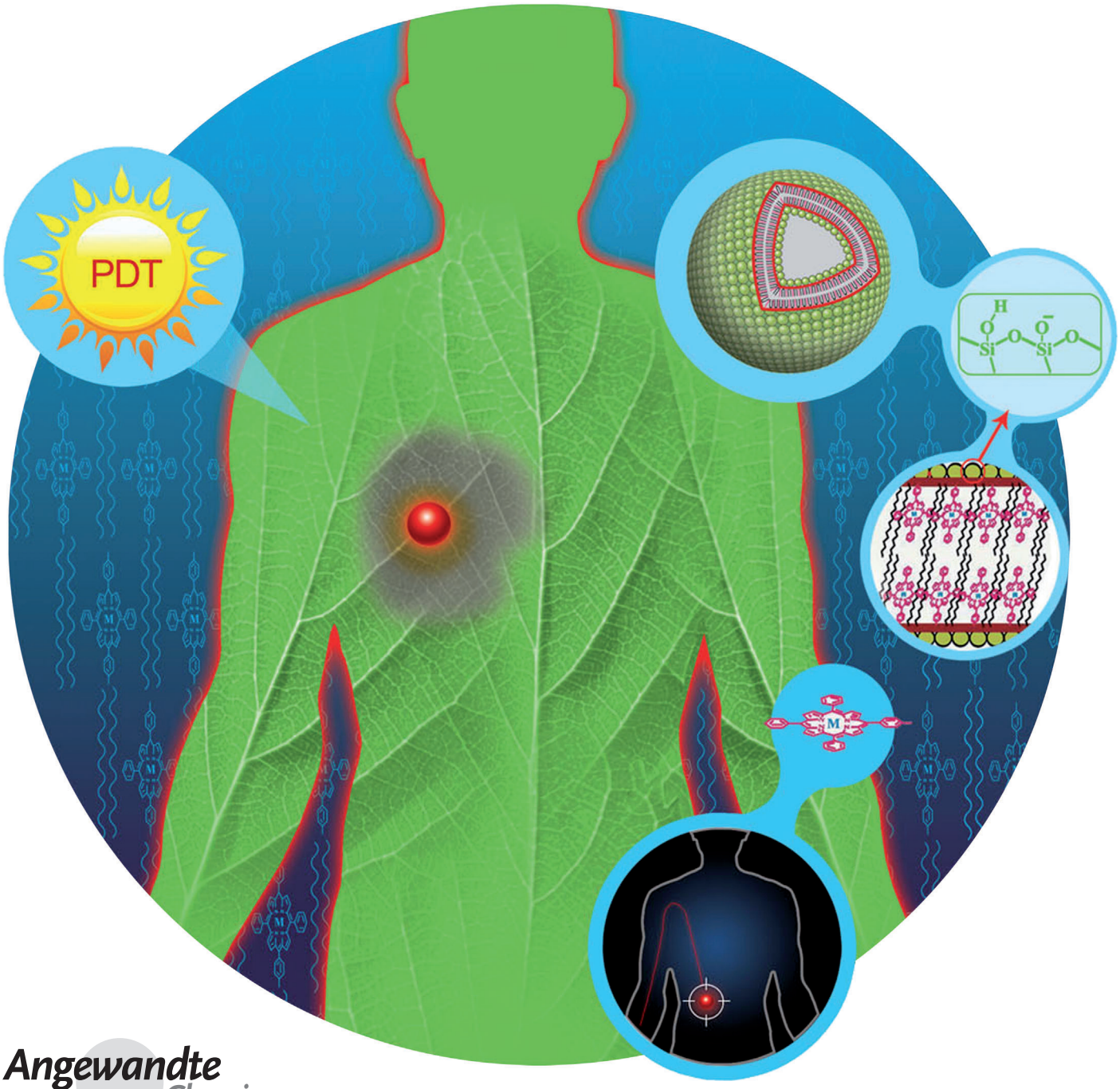

Photodynamic therapy (PDT) is an emerging treatment for eradicating premalignant and early-stage cancer and reducing the tumor size in end-stage cancers by photosensitizers (PSs).[1–3] When PSs are exposed to light of appropriate wavelength, they produce highly reactive oxygen species (ROS) that cause an effective and selective destruction of diseased tissues without damage to the surrounding healthy tissues.[4–8] However, most photosensitizers that are used clinically or in preclinical development are hydrophobic and strongly aggregate in aqueous media.[9] This aggregation significantly reduces their photosensitizing efficacy because only monomeric species are appreciably photoactive.[9] Many types of nanocarries, such as polymeric micelles, conjugated polymer nanoparticles, and silica nanoparticles have been extensively used to fabricate a stable dispersion of PDT drugs in aqueous systems.[10–14] However, most of them suffer from poor drug loading or increased self-aggregation of the drug in the entrapped state.

With the aim of improving the efficacy and safety of PDT, liposomes with their versatility in accommodating PSs of different physicochemical properties, came into focus as a valuable carrier and delivery system.[9,15] However, the insufficient morphological stability of the conventional liposomes may lead to rapid clearance of the vesicles from circulation before reaching their target. For example, a lipid exchange between the liposomes and lipoproteins leads to an irreversible disintegration of the liposome.[15] The fast disintegration process releases PSs in the bloodstream. This premature release results in a reduced efficacy of treatment because the release of the PS drugs is not a prerequisite for PDT action unlike conventional chemotherapy.[10,11] In addition, in liposomes the drug contents are generally less than 10%. Therefore, highly stable liposomes with a high PS loading efficiency offer a better prospect in becoming carriers of photosensitizers.

Porphyrins are the most popular PSs for PDT. Porphyrin-loaded liposomes have been described for PDT applications, but they can accommodate only a small fraction of porphyrin molecules.[9] Recently, the so-called porphysomes, self-assembled from phospholipid–porphyrin conjugates that exhibit a liposome-like structure and high absorption of near-infrared light, have been reported.[16] As porphysomes are highly self-quenched, they show promise for diverse biophotonic imaging applications and photothermal therapy. But porphysomes exhibit almost no photosensitizing effect because the energy that is normally released to fluorescence and singlet-oxygen generation is dissipated thermally.

Herein, we fabricated porphyrin bilayer cerasomes (PBCs) for the first time by sol–gel and self-assembly processes from a conjugate of porphyrin-organoalkoxysilylated lipids (PORSILs) with two triethoxysilyl groups, a hydrophobic double-chain segment, a porphyrin moiety, and a connecting unit (Figure 1). Compared with the reported cerasomes,[17] the covalent linkage of porphyrin to cerasomes may result in a drug loading content of 33.46% in the PBCs. This loading is significantly higher than that of physically entrapping cerasomes or liposomes (generally less than 10%). In addition, the premature release of PSs can be avoided during systemic circulation.

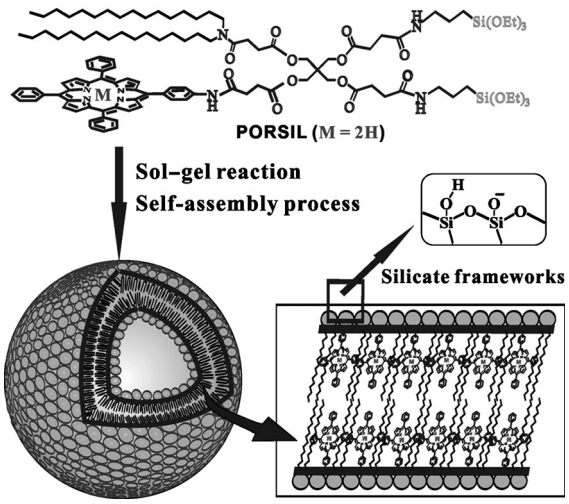

Figure 1. Formation of PBCs from a PORSIL lipid.

Our basic idea for the synthesis of a bilayer-forming lipid is to couple both silica precursor and porphyrin units to a lipid that contains several functional groups. In this respect, one of the major issues is the multifunctional core. Therefore, multivalent pentaerythritol is used for conjugation with different target structures because it is readily available and its four primary hydroxy groups are symmetric and highly reactive. A protecting–deprotecting strategy is applied for the synthesis of the PORSIL lipid, as shown in Scheme S1 in the Supporting Information. Excess-protected pentaerythritol **2**[18] was first coupled with compound **1**[17c] to give **3** bearing a hydroxy group, which reacted with succinic anhydride followed by a deprotection step to obtain intermediate **5** with two hydroxy and one carboxy groups. Then, the latter group was selectively coupled with 5-(4-aminophenyl)-10,15,20-triphenylporphyrin catalyzed by *N*-(3-dimethylaminopropyl)-*N*-ethylcarbodiimide (EDC) to afford **7**. Then, its remaining two hydroxy arms were reacted with succinic anhydride. Finally, the resultant scaffold **8** with two free carboxy groups was coupled to 3-aminopropyltriethoxylsilane (APTES) through simple amide linkages to obtain the targeting PORSIL lipid. For the preparation and characterization of the above-mentioned compounds see the Supporting Information.

[*] X. Liang, X. Li, Prof. X. Yue, Prof. Z. Dai
Nanomedicine and Biosensor Laboratory, School of Sciences
State Key Laboratory of Urban Water Resources and Environment
Harbin Institute of Technology, Harbin, 150001 (P.R. China)
E-mail: zhifei.dai@hit.edu.cn
Homepage: http://nanobio.hit.edu.cn/

[**] This research was financially supported by the National Natural Science Foundation of China (grant numbers NSFC-30970829 and 20977021).

Supporting information for this article is available on the WWW under http://dx.doi.org/10.1002/anie.201103557.

The PORSIL lipid was dispersed in water by ultrasonication, resulting in the formation of vesicles which self-rigidified through in situ sol–gel processes ($Si{-}OCH_2CH_3 + H_2O \rightarrow Si{-}OH + CH_3CH_2OH$ followed by $2Si{-}OH \rightarrow Si{-}O{-}Si + H_2O$) on the vesicular surface.[17] Transmission electron microscopic (TEM) images clearly showed the formation of spherical vesicles with a diameter range from 50 to 100 nm (Figure 2a), which is in agreement with dynamic light scattering (DLS)

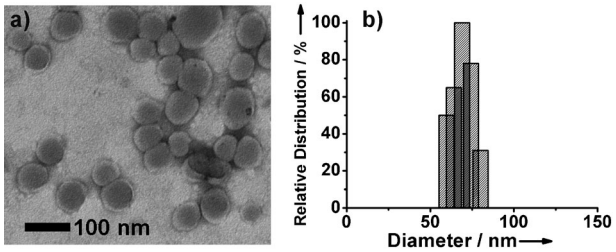

Figure 2. a) TEM micrograph of PBCs. b) Dynamic light scattering measurement of PBCs in H_2O.

measurements that gave a sharp peak with a narrow distribution at (70 ± 13) nm (Figure 2b). The vesicular structure of PBCs was further confirmed by encapsulation of a water-soluble fluorescent dye of calcein. The calcein-loaded vesicles had brightly green-fluorescent cores and red-fluorescent shells, which we could clearly observe by confocal laser scanning microscopy (CLSM; see Figure S1 in the Supporting Information). The red emission resulted from the conjugated porphyrin in the lipid bilayer of PBCs and the green emission from calcein in the aqueous core of PBCs. Thus, the capability to load water-soluble compounds into the core of PBCs proved the existence of a vesicular structure. The formation of siloxane bonds on the surface of PBCs was proved by Fourier transform infrared (FT-IR) spectroscopy (see Figure S2 in the Supporting Information). Stretching bands assigned to Si–O–Si and Si–OH groups were observed around 1100 and 950 cm^{-1}, respectively. The former peak intensity was much stronger than the latter, suggesting that PBCs had a silica-like surface with siloxane frameworks and a high degree of polymerization.

The morphological stability of PBCs was evaluated using surfactant dissolution experiments. Although five equivalents of nonionic surfactant Triton X-100 can completely destroy the conventional liposomes from distearoyl phosphatidylcholine (DSPC), almost no change was observed for the hydrodynamic diameter of the PBCs, even in the presence of 35 equivalents of Triton X-100 after incubation for 24 h (see Figure S3 in the Supporting Information). Such remarkable morphological stability of the PBCs was attributed to the development of a siloxane network on the vesicular surface.

To confirm that porphyrins are conjugated with PBCs, both PORSIL lipids and PBCs have been applied onto silica thin layer chromatography (silica-TLC) plates in developing agent of ethyl acetate (see Figure S4 in the Supporting Information).[11] Free porphyrin (see Figure S5 in the Supporting Information) and the porphyrin-entrapped cerasomes from an organoalkoxysilylated lipid (see Figure S6 in the Supporting Information) were used as control. The control cerasome, in which porphyrins were just physically encapsulated, is eluted similarly to free porphyrin molecules in the direction of the solvent front. In contrast, PBCs remain at the bottom. The physically encapsulated porphyrin molecules can be easily extracted from the cerasomes by organic solvent while the porphyrins conjugated to PBCs are not able to be washed off because of the covalent linkage.

Compared with PORSIL lipids in chloroform, the UV/Vis absorption spectra of PBCs broadened and the absorbance of PBCs increased but the formation of cerasomes did not have a major effect on the position of the Soret and Q bands of porphyrin (Figure 3A). The shape of the absorption spectrum of PBCs is quite similar to that of the solution-phase PORSIL lipid. This similarity indicates that aggregation does not occur

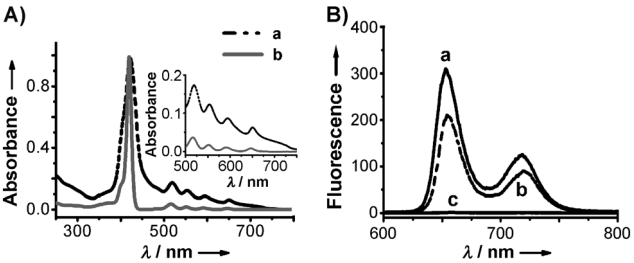

Figure 3. A) Absorption spectra of a) PBCs in water and b) PORSIL in chloroform. B) Fluorescence spectra under excitation with light of 419 nm: a) PORSIL in chloroform, b) PBCs in water, and c) free porphyrin in DMF/water (0.2%). The excitation and emission slit widths were both set at 10 nm, and all samples had the same porphyrin concentration of 15 μM.

in the nanoparticles. Both Soret and Q bands display a bathochromic shift of 3 nm because of the arrangement of the porphyrin groups and alkyl chains in the lipid bilayer membrane. The existence of double-alkyl chains sterically hinders porphyrin moieties to approach each other, which can greatly reduce the aggregation of the porphyrin moieties. Therefore, we believe this method is highly effective for the preparation of photofunctional cerasomes without aggregation or reduced photoluminescent quality.

Figure 3B shows the fluorescence emission spectra of PORSIL lipid in chloroform (Figure 3Ba) and the aqueous dispersion of PBC vesicles (Figure 3Bb) at the same concentration of porphyrin, which was determined by UV/Vis absorption spectra (see Figure S7 in the Supporting Information). The aqueous PBC vesicles were clearly fluorescent upon light irradiation (see Figure S8 in the Supporting Information). At the same concentration of porphyrin, the fluorescence intensity of the aqueous PBCs is about 32% lower than the PORSIL lipid in chloroform, but much higher than free porphyrin (see Figure S5 in the Supporting Information) in 0.2% DMF/water, which shows practically no emission (Figure 3Bc). This absence of fluorescence may be due to either porphyrin–solvent interactions promoting nonradiative decay or self-aggregation of porphyrin molecules. PBCs show a remarkably stronger fluorescence in aqueous media than free porphyrin, which permits the use of PBCs as

fluorescent nanoprobes for biological applications. PBCs are very different from the reported porphysomes, which showed almost complete fluorescent self-quenching because of an energetically favorable supramolecular structure, in which the orientation of the constituents of porphyrin and lysophosphatidylcholine facilitate extensive porphyrin interactions and quenching.[16] The porphysome subunits consisted of a hydrophobic porphyrin and a single alkyl chain. In contrast, the PBCs subunits consisted of a hydrophobic porphyrin and two alkyl chains and the presence of the two alkyl chains prevented porphyrins from aggregating, avoiding significant fluorescent self-quenching of the PBCs.

The generation of singlet oxygen by PBCs was detected chemically using the disodium salt of 9,10-anthracenedipropionic acid (ADPA) as a detector, which was bleached to its nonfluorescent endoperoxide in the presence of $^1O_2$.[19] Figure 4A,B shows the decrease in optical density (OD) at 378 nm as a function of irradiation time. In the case of the PBCs (Figure 4A and 4Ba), the sharp decrease of the ADPA absorbance with irradiation time confirmed the $^1O_2$ generation from PBCs. Nevertheless, the ADPA absorbance decreased much slower in the presence of free porphyrin (Figure 4Bb and Figure S9 in the Supporting Information), indicating that the free porphyrin had a much lower capability to generate $^1O_2$ than PBCs. The conjugation of porphyrin to cerasomes can significantly improve the $^1O_2$ generation. In stark contrast, the cerasome without porphyrin unit (Figure 4Bc) produced no change in the OD of ADPA under light irradiation, further confirming that the bleaching of ADPA in the presence of porphyrin is caused by singlet oxygen and not by the irradiated light.

The $^1O_2$ generation in D_2O solution was further detected by ESR spectroscopy using 2,2,6,6-tetramethyl-4-piperidone (TEMP) as a spin-trapping agent, which is selective for $^1O_2$.[20] Figure S10 in the Supporting Information shows that the ESR signal intensity of both free porphyrin and PBCs increased linearly as the irradiation time increased whereas the signal intensity of PBCs increased more significantly than that of free porphyrin. In contrast, no ESR signal was observed without light irradiation, proving the inactivity of PSs in the dark. After irradiation of cells incubated with PSs, the $^1O_2$ generation was characterized by ESR spin trapping using α-(4-pyridyl-1-oxide)-*N*-tert-butylnitrone (POBN) combined with ethanol (2%).[21] As shown in Figures S11 and S12 in the Supporting Information, upon light irradiation, the ESR spectrum appeared to be a triple double-lined spectrum, representing the presence of POBN-ethoxy adducts. The ESR signal intensity was found to increase with increasing PSs concentration and irradiation time (Figure 4C,D). Upon addition of 1,4-diazabicyclo[2.2.2]octane (DABCO), a specific quencher of $^1O_2$, the POBN-ethoxy adduct signal intensity almost disappeared (see Figure S12Bf in the Supporting Information), further confirming the generation of $^1O_2$ in cells. The comparison of ESR spectra obtained with free porphyrin and PBCs revealed that the conjugation of a porphyrin molecule to cerasomes led to higher efficiency of $^1O_2$ generation. These findings were in good agreement with the results shown in Figure 4B.

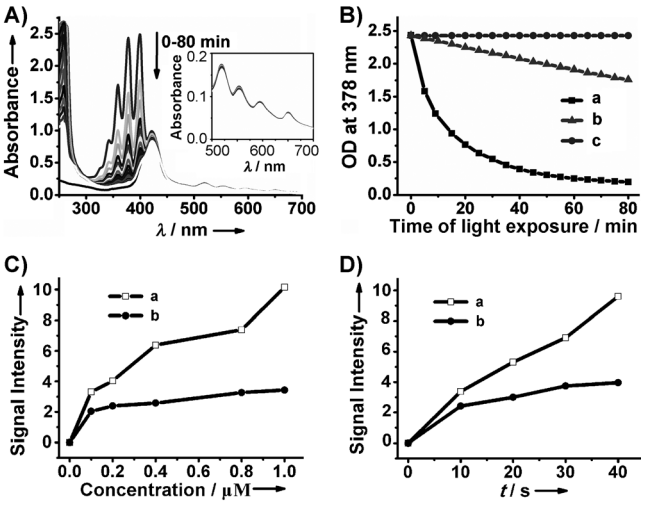

Figure 4. A) Time-dependent bleaching of ADPA caused by singlet oxygen generated by PBCs. B) The change in ADPA absorption at 378 nm as a function of the time of light exposure: a) PBCs, b) free porphyrin (1%, DMSO/D_2O), and c) cerasome without a porphyrin unit. C) Concentration-dependent increase of ESR signal intensity in HeLa cells (irradiation for 60 s): a) PBCs and b) free porphyrin. D) Time-dependent increase of ESR signal intensity in HeLa cells: a) PBCs (5 μM) and b) free porphyrin (5 μM).

Irradiation of the PBCs with light of suitable wavelength results in the efficient generation of singlet oxygen, which is possible because of the inherent porosity of the nanoparticles. The siloxane network is not so highly developed on the PBCs surface because the length of the Si–O–Si bond is much shorter than the diameter of the cross-section of the double-chain segment and the porphyrin moiety of the amphiphiles, which takes the molecular packing of the stable bilayer structure into account. This effect perturbs the membrane structure and may induce the formation of pores. Under irradiation the photosensitizing porphyrin units within the PBCs can interact with molecular oxygen which has diffused through the pores. This can lead to the formation of singlet oxygen by energy transfer from the excited photosensitizer to molecular oxygen, which can then diffuse out of the PBCs to produce a cytotoxic effect in the tumor cells.

CLSM was used to verify the cellular localization of PBCs (Figure 5). Fluorescent PBCs were clearly observed inside the cells as red spots distributed in the cytoplasm and mainly localized in the lysosomes. An almost complete co-localization could be observed between red and green fluorescence as it was evident from the pale yellow fluorescence arising from the overlap of the two fluorescence images. After the nuclei of the tumor cells were stained with 4′,6-diamidino-2-phenylindole (DAPI; blue in Figure 5c), PBCs were found to be distributed throughout the entire cytoplasm (Figure 5d), indicating that PBCs were indeed endocytosed as reported previously on the cellular uptake of cerasomes.[22] After the cells were treated by sucrose and K^+-free buffer the uptake of cerasomes by cells decreased to 73 and 75%, respectively, suggesting that the uptake of PBCs occurred possibly through a clathrin-dependent endocytosis pathway.[22] Silica nanoparticles could be endocytosed partially due to their strong affinity to the head-groups of a variety of phospholipids and

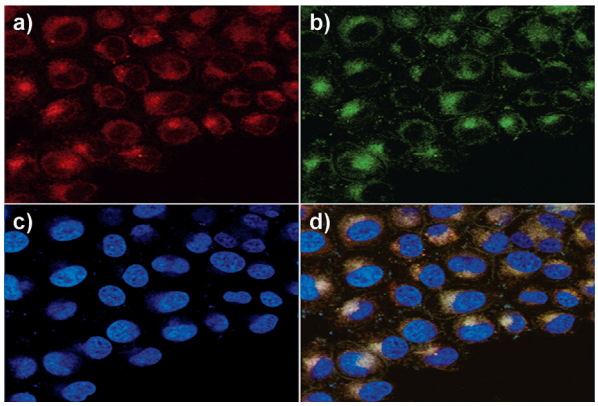

Figure 5. Subcellular localization of PBCs observed by fluorescent CLSM. HeLa cells were incubated with PBCs at a concentration of 5 μM for 4 h at 37 °C. Observations of a) the PBCs channel, b) LysoTracker green (DND-26, to label lysosomes) channel, c) the nuclear dye DAPI channel, and d) the overlap of the above images.

clathrin-coated vesicles. This suggests that the similar surface properties of PBCs and silica nanoparticles may facilitate their adhesion to the cell membrane and their subsequent uptake. Therefore, the high affinity to cell surfaces, which eventually leads to endocytosis of PBCs with silica surface, is not surprising.[23]

In in vitro PDT tests bright field images and fluorescence images of HeLa cells were taken to monitor cell viability. Images of HeLa cells before and after photoirradiation using a xenon lamp equipped with a VIS mirror module at wavelengths of 400–700 nm for 10 min are shown in Figure 6 A,a,c and Figure 6 A,b,d, respectively. After treatment with 0.2 μM PBCs followed by 10 min of irradiation and 24 h of incubation, significant damage to the impregnated HeLa cells could be clearly observed and the cells displayed shrinkage and deformation (Figure 6 A,b). Cell survival was then determined with calcein AM, a fluorescence dye that stains the cell green when the cell is still living. As shown in Figure 6 A,d, the number of living cells decreased greatly. In contrast, the control experiments without light irradiation showed that PBCs alone did not cause cell death (Figure 6 A,c). These experiments indicated the significant phototoxicity of PBCs.

The cell phototoxicity study, represented in Figure 6 B, shows the percentage of cell survival after treatment of HeLa cells at various concentrations of PBCs followed by subsequent irradiation with light (400–700 nm).[24] Significant phototoxic effect on the cultured cells can be observed. In addition, the uptake amount of PBCs increased with the elevated concentration, further leading to a higher phototoxicity against HeLa cells. In contrast, after 24 h of incubation, no significant decrease in cell viability in the dark could be observed at concentrations of PBCs below 1.0 μM, indicating low dark toxicity of PBCs. These data were well consistent with the results of cell images (Figure 6 A). Nevertheless, free porphyrin molecules showed higher dark toxicity and remarkably lower phototoxicity relative to that of PBCs. As shown in Figure S13 in the Supporting Information, no apparent phototoxicity was observed at concentrations below

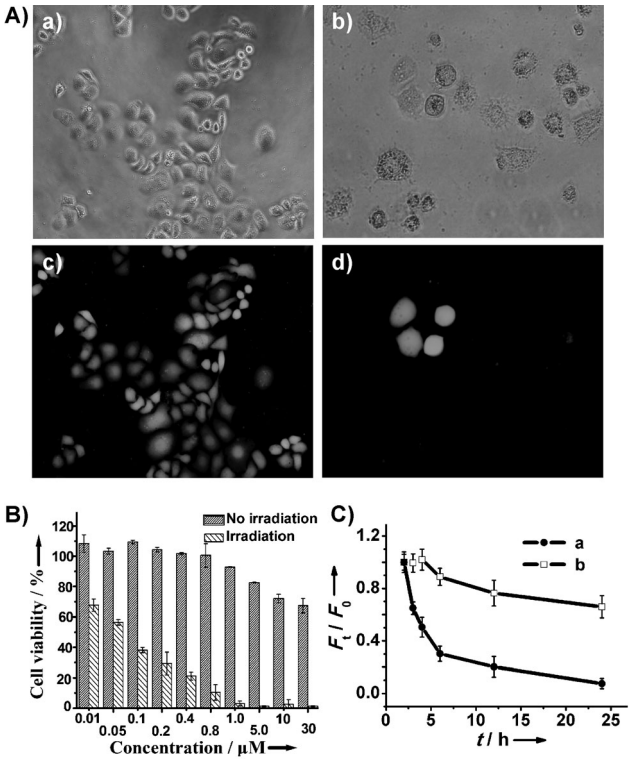

Figure 6. A) Fluorescence microscopic observations of HeLa cells treated with 0.2 μM PBCs and stained with calcein AM. a,b) Bright-field images. c,d) Fluorescence images. a,c) Before irradiation. b,d) After irradiation with light of 400–700 nm for 10 min followed by 24 h of incubation at 37 °C in the dark. B) HeLa cell viability at different concentrations of PBCs with or without irradiation for 10 min with reference to the irradiated but untreated cells. The cell viability was assayed by the MTT method (values: mean value ± standard deviation). C) Change in the blood fluorescence of a) PLLs and b) PBCs ($n = 3$). Fluorescence intensities F_0 and F_t of the porphyrin molecule at the initial and the given time, respectively.

1.0 μM. When the concentration was above 5.0 μM, the cell viability decreased, mainly arising from the dark toxicity of the free drug. These results were in good accordance with the singlet oxygen generation data, further confirming the potential of PBCs for destroying tumor cells by light exposure.

The blood circulation dynamics of PBCs was investigated and compared to that of the porphyrin-loaded DSPC liposomes (PLLs). The blood fluorescence intensity of PLLs decreased to 30 % after 6 h and almost no fluorescence was observed after 24 h, exhibiting rapid clearance kinetics (Figure 6 C a). On the contrary, the decrease in the blood fluorescence intensity of PBCs was only 33.5 % at 24 h, showing dramatically prolonged and slow clearance kinetics (Figure 6 C b). Values of elimination half-life ($t_{1/2}$) and area under the plasma concentration–time curve from 0 to 24 h ($AUC_{0\text{-}24}$) for PBCs were calculated to be (38.04 ± 5.68) h and (726.84 ± 61.38) μg h mL^{-1}, respectively. In contrast, the $t_{1/2}$ and $AUC_{0\text{-}24}$ of PLLs were (8.18 ± 0.69) h and (264.53 ± 32.96) μg h mL^{-1}. Thus, evidence was provided that PBCs can maintain a long circulation without PEG chains.

In conclusion, we have successfully developed a cerasomal photosensitizers by chemical conjugation of porphyrin to an organoalkoxysilylated lipid. We showed that it is convenient to regulate the optical density bands of the vesicles to the desired operating wavelengths by inserting metal ions into the porphyrin moiety or replacing porphyrin molecules with other types of photosensitizers. The silica-like surface endows the PBCs with a remarkably high stability whereas the inherent porosity allows oxygen molecules to diffuse in and out of the vesicles freely. In addition, the drug loading efficiency of PBCs (33.46%) is significantly higher than that of the physical entrapment of cerasomes. The covalent linkage of porphyrins can prevent cerasomes to release PSs during systemic circulation and thus enhances the outcome of PDT. The proper arrangement of porphyrins in the lipid bilayer ensures the efficacy of singlet oxygen production. Even at an extremely high number of porphyrins, fluorescence loss of the porphyrins is effectively prevented, resulting in a powerful tool for in vivo imaging and photodynamic diagnostics. The capability to load chemotherapy drugs in the internal aqueous core of PBCs makes it possible to develop drug–carrier systems for the synergistic combination of chemotherapy and PDT for the treatment of cancer. The PBCs are avidly taken up by malignant cells and show cellular phototoxicity under irradiation. There is no doubt that PBCs will play an important role in clinical photodynamics.

Received: May 24, 2011
Revised: September 24, 2011
Published online: October 14, 2011

Keywords: cancer · liposomes · photodynamic therapy · self-assembly · sol–gel processes

[1] W. M. Sharman, C. M. Allen, J. E. van Lier, *Drug Discovery Today* **1999**, *4*, 507 – 517.
[2] Z. Huang, *Technol. Cancer Res. Treat.* **2005**, *4*, 283 – 294.
[3] D. E. J. G. J. Dolmans, D. Fukumura, R. K. Jain, *Nat. Rev. Cancer* **2003**, *3*, 380 – 387.
[4] Y. N. Konan, R. Gruny, E. Allemann, *J. Photochem. Photobiol. B* **2002**, *66*, 89 – 106.
[5] T. Dougherty, C. Gomer, B. Henderson, G. Jori, D. Kessel, M. Korbelik, J. Moan, Q. Peng, *J. Natl. Cancer Inst.* **1998**, *90*, 889 – 905.
[6] J. F. Lovell, T. W. B. Liu, J. Chen, G. Zheng, *Chem. Rev.* **2010**, *110*, 2839 – 2857.
[7] P. N. Prasad, *Introduction to Biophotonics*, Wiley, New York, **2003**.
[8] B. C. Wilson, M. S. Patterson, *Phys. Med. Biol.* **2008**, *53*, R61 – R109.
[9] B. Chen, B. W. Pogue, T. Hasan, *Expert Opin. Drug Delivery* **2005**, *2*, 477 – 487.
[10] I. Roy, T. Y. Ohulchanskyy, H. E. Pudavar, J. E. Bergey, A. R. Oseroff, J. Morgan, T. J. Dougherty, P. N. Prasad, *J. Am. Chem. Soc.* **2003**, *125*, 7860 – 7865.
[11] T. Y. Ohulchanskyy, I. Roy, L. N. Goswami, Y. Chen, E. J. Bergey, R. K. Pandey, A. R. Oseroff, P. N. Prasad, *Nano Lett.* **2007**, *7*, 2835 – 2842.
[12] C. F. van Nostrum, *Adv. Drug Delivery Rev.* **2004**, *56*, 9 – 16.
[13] S. Wang, R. Gao, F. Zhou, M. Selke, *J. Mater. Chem.* **2004**, *14*, 487 – 493.
[14] D. Gao, R. R. Agayan, H. Xu, M. A. Philbert, R. Kopelman, *Nano Lett.* **2006**, *6*, 2383 – 2386.
[15] A. S. L. Derycke, P. A. M. de Witte, *Adv. Drug Delivery Rev.* **2004**, *56*, 17- 30.
[16] J. F. Lovell, C. S. Jin, E. Huynh, H. Jin, C. Kim, J. L. Rubinstein, W. C. W. Chan, W. Cao, L. V. Wang, G. Zheng, *Nat. Mater.* **2011**, *10*, 324 – 332.
[17] a) Z. Dai, W. Tian, X. Yue, Z. Zheng, J. Qi, N. Tamai, J. Kikuchi, *Chem. Commun.* **2009**, 2032 – 2034; b) Z. Cao, Y. Ma, X. Yue, S. Li, Z. Dai, J. Kikuchi, *Chem. Commun.* **2010**, *46*, 5265 – 5267; c) K. Katagiri, M. Hashizume, K. Ariga, T. Terashima, J. Kikuchi, *Chem. Eur. J.* **2007**, *13*, 5272 – 5281; d) X. Liang, X. Yue, Z. Dai, J. Kikuch, *Chem. Commun.* **2011**, *47*, 4751 – 4753.
[18] "Monobenzalpentaerythritol": C. H. Issidorides, R. C. Gulen in *Organic Syntheses Collected Volume IV* (Ed.: N. d. Rabjohn, Wiley, New York, **1963**, p. 679.
[19] B. A. Lindig, M. A. J. Rodgers, A. P. Schaap, *J. Am. Chem. Soc.* **1980**, *102*, 5590 – 5593.
[20] S. Dzwigaj, H. Pezerat, *Free Radical Res.* **1995**, *23*, 103 – 115.
[21] P.-H. Guelluy, M.-P. Fontaine-Aupart, A. Grammenos, S. Lécart, J. Pietted, M. Hoebekea, *Photochem. Photobiol. Sci.* **2010**, *9*, 1252 – 1260.
[22] Y. Ma, Z. Dai, Y. Gao, Z. Cao, Z. Zha, X. Yue, J. Kikuchi, *Nanotoxicology* **2011**, DOI: 10.3109/17435390.2010.546950.
[23] a) X. L. Huang, X. Teng, D. Chen, F. Q. Tang, J. Q. He, *Biomaterials* **2010**, *31*, 438 – 448; b) S. Mornet, O. Lambert, E. Duguet, A. Brisson, *Nano Lett.* **2005**, *5*, 281 – 285.
[24] R. Ideta, F. Tasaka, W.-D. Jang, N. Nishiyama, G.-D. Zhang, A. Harada, Y. Yanagi, Y. Tamaki, T. Aida, K. Kataoka, *Nano Lett.* **2005**, *5*, 2426 – 2431.

